ROYAL SOCIETY
OF CHEMISTRY

PAPER

Check for updates

Efficiency of liquid tin(II) *n*-alkoxide initiators in the ring-opening polymerization of L-lactide: kinetic studies by non-isothermal differential scanning calorimetry†

Montira Sriyai, [ID] [abc] Tawan Chaiwon,[ac] Robert Molloy,[d] Puttinan Meepowpan [ID] [abd] and Winita Punyodom [ID] *[abd]

Novel soluble liquid tin(II) *n*-butoxide ($Sn(OnC_4H_9)_2$), tin(II) *n*-hexoxide ($Sn(OnC_6H_{13})_2$), and tin(II) *n*-octoxide ($Sn(OnC_8H_{17})_2$) initiators were synthesized for use as coordination–insertion initiators in the bulk ring-opening polymerization (ROP) of L-lactide (LLA). In order to compare their efficiencies with the more commonly used tin(II) 2-ethylhexanoate (stannous octoate, $Sn(Oct)_2$) and conventional tin(II) octoate/*n*-alcohol ($SnOct_2/nROH$) initiating systems, kinetic parameters derived from monomer conversion data were obtained from non-isothermal differential scanning calorimetry (DSC). In this work, the three non-isothermal DSC kinetic approaches including dynamic (Kissinger, Flynn–Wall, and Ozawa); isoconversional (Friedman, Kissinger–Akahira–Sunose (KAS) and Ozawa–Flynn–Wall (OFW)); and Borchardt and Daniels (B/D) methods of data analysis were compared. The kinetic results showed that, under the same conditions, the rate of polymerization for the 7 initiators/initiating systems was in the order of liquid $Sn(OnC_4H_9)_2 > Sn(Oct)_2/nC_4H_9OH > Sn(Oct)_2 \cong$ liquid $Sn(OnC_6H_{13})_2 > Sn(Oct)_2/nC_6H_{13}OH \cong$ liquid $Sn(OnC_8H_{17})_2 > Sn(Oct)_2/nC_8H_{17}OH$. The lowest activation energies ($E_a = 52$, 59, and 56 kJ mol^{-1} for the Kissinger, Flynn–Wall, and Ozawa dynamic methods; $E_a = 53–60$, 55–58, and 60–62 kJ mol^{-1} for the Friedman, KAS, and OFW isoconversional methods; and $E_a = 76–84$ kJ mol^{-1} for the B/D) were found in the polymerizations using the novel liquid $Sn(OnC_4H_9)_2$ as the initiator, thereby showing it to be the most efficient initiator in the ROP of L-lactide.

1. Introduction

Biodegradable aliphatic polyesters have attracted much interest as replacements for petroleum-based materials due to their environmentally friendly properties and derivability from renewable resources. The most popular and important biodegradable aliphatic polyesters are poly(L-lactide) (PLLA), polyglycolide (PGA), poly(ε-caprolactone) (PCL), and their other high molecular weight co- or terpolymers. Among these, PLA-based materials are of the most interest due to their biocompatibility and biodegradability in a broad range of applications, especially biomedical applications such as absorbable surgical sutures, controlled drug delivery systems, and bone fixation

[a]Department of Chemistry, Faculty of Science, Chiang Mai University, Chiang Mai 50200, Thailand

[b]Center of Excellence for Innovation in Chemistry (PERCH-CIC), Faculty of Science, Chiang Mai University, Chiang Mai 50200, Thailand

[c]Graduate School, Chiang Mai University, Chiang Mai 50200, Thailand

[d]Center of Excellence in Materials Science and Technology, Chiang Mai University, Chiang Mai 50200, Thailand. E-mail: winitacmu@gmail.com

† Electronic supplementary information (ESI) available. See DOI: 10.1039/d0ra07635j

devices.[1–5] Poly(lactic acid) (PLA) can be produced from lactic acid derived from the fermentation of renewable starch-containing resources such as corn, sugar beet, and cassava.[6–8] Lactide (L) monomer is prepared by condensing lactic acid to low molecular weight PLA which is then thermally cracked to yield the six-membered ring lactide monomer. The crude lactide monomer can be purified by repeated recrystallization before being polymerized in bulk to form high molecular weight PLA.[9]

Tin(II) 2-ethylhexanoate or stannous octoate ($Sn(Oct)_2$) is the most common initiator used in the ROP of lactones and lactides due to its effectiveness and versatility. It is also easy to handle and is soluble in most common organic solvents and monomers.[10–12] Moreover, it has been approved for use as a food additive by the US Food and Drug Administration (FDA). However, in order to improve its effectiveness, $Sn(Oct)_2$ is usually used in combination with an alcohol co-initiator (ROH) as the initiating system.

Mechanistically, Kricheldorf and co-workers proposed the coordination of the $Sn(Oct)_2$ and the alcohol with the cyclic ester monomer followed by ROP.[13] In this mechanism, the $Sn(Oct)_2$ serves as a catalyst while the alcohol is an initiator, as depicted in Fig. 1(a). However, Penczek *et al.* later suggested
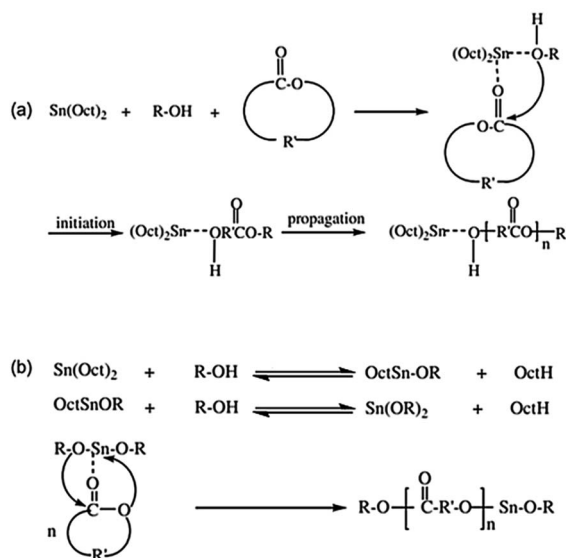
Paper

Fig. 1 Comparison of the old (a) and the new (b) mechanistic proposals using Sn(Oct)$_2$: (a) complexation of the monomer and alcohol prior to ROP and (b) formation of tin(II) alkoxide before ROP.[13,14]

that the Sn(Oct)$_2$ and the alcohol react together resulting in the formation of a tin(II) monoalkoxide ((Oct)Sn(OR)) and tin(II) dialkoxide (Sn(OR)$_2$) which then become the 'true' initiators as shown in Fig. 1(b).[14] This latter mechanism is now widely accepted as the true initiation pathway. Therefore, in order to produce high molecular weight polyesters *via* ROP, it is vitally important to know the exact concentration of the tin(II) alkoxide initiator which should be easily and completely soluble in the cyclic ester monomer.

As previously mentioned, it is now widely accepted that the tin(II) monoalkoxide, (Oct)Sn(OR), and/or the dialkoxide, Sn(OR)$_2$, are the true initiators formed *in situ via* the reaction between Sn(Oct)$_2$ and ROH. Since the coupled reactions in Fig. 1(b) are both reversible and interdependent, the exact initiator concentrations will be unknown. Moreover, stannous octoate is well known to be an effective transesterification catalyst, ROH can act as a chain transfer agent, and the octanoic acid (OctH) by-product can also catalyze other unwanted side-reactions. Thus, the kinetics of the ROP and the final molecular weight of the polymer cannot be accurately predicted. Therefore, in order to overcome this problem, it is logical to synthesize the tin(II) dialkoxide (Sn(OR)$_2$) separately so that it can be used directly in an accurately known concentration.
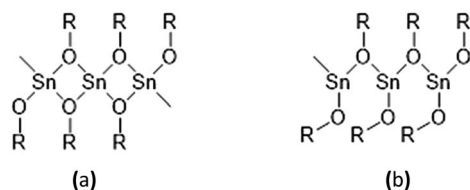

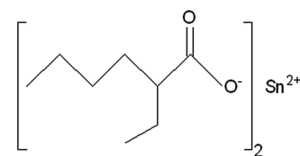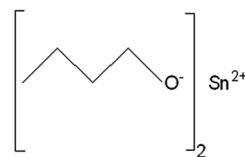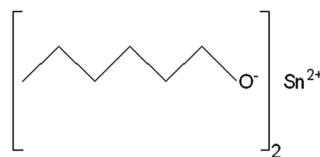Fig. 2 Molecular self-aggregations in solid tin(II) alkoxides: (a) angular aggregation and (b) linear aggregation.

tin)II(octoate, Sn)C$_8$H$_{15}$O$_2$($_2$

tin)II(*n*-butoxide, Sn)O*n*C$_4$H$_9$($_2$

tin)II(*n*-hexoxide, Sn)O*n*C$_6$H$_{13}$($_2$

tin)II(*n*-octoxide, Sn)O*n*C$_8$H$_{17}$($_2$

Fig. 3 Chemical structures of: tin(II) octoate; tin(II) *n*-butoxide; tin(II) *n*-hexoxide; and tin(II) *n*-octoxide initiators.

The synthesis of solid tin(II) alkoxides has been known for over 50 years.[15,16] However, they have been found to have their drawbacks as initiators, in particular their difficult solubility in cyclic ester monomers and common organic solvents and their instability in contact with air and moisture which is caused by
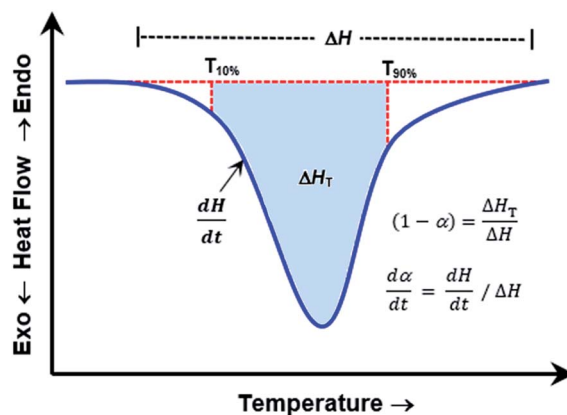

Fig. 4 Idealized DSC curve for kinetic parameters determination by using Borchardt and Daniels (B/D) method.

Table 1 Polymer codes and conditions used in the ROP of L-lactide using liquid $Sn(OnC_4H_9)_2$ as an initiator

Polymer code	$[Sn(OnC_4H_9)_2]$ (mol%)	Temperature (°C)	Polymerization time (h)
PLLA 1	0.01	100	24
PLLA 2	0.01	110	24
PLLA 3	0.01	120	24
PLLA 4	0.01	130	24
PLLA 5	0.01	140	24
PLLA 6	0.01	150	24
PLLA 7	0.05	100	24
PLLA 8	0.05	110	24
PLLA 9	0.05	120	24
PLLA 10	0.05	130	24
PLLA 11	0.05	140	24
PLLA 12	0.05	150	24
PLLA 13	0.10	100	24
PLLA 14	0.10	110	24
PLLA 15	0.10	120	24
PLLA 16	0.10	130	24
PLLA 17	0.10	140	24
PLLA 18	0.10	150	24
PLLA 19	0.50	100	24
PLLA 20	0.50	110	24
PLLA 21	0.50	120	24
PLLA 22	0.50	130	24
PLLA 23	0.50	140	24
PLLA 24	0.50	150	24
PLLA 25	1.00	100	24
PLLA 26	1.00	110	24
PLLA 27	1.00	120	24
PLLA 28	1.00	130	24
PLLA 29	1.00	140	24
PLLA 30	1.00	150	24

their solid-state molecular self-aggregations as shown in Fig. 2(a) and (b). According to their low solubility in most organic solvents and cyclic ester monomers of these solid tin(II) alkoxides, the polymerizations of monomers such as L-lactide, D-lactide, DL-lactide, ε-caprolactone and other cyclic esters are relatively slow and ineffective.

Consequently, in this work, some novel liquid soluble tin(II) alkoxides were prepared for use in the ROP of L-lactide in order to overcome the molecular self-aggregation difficulties found in previous works with solid tin(II) alkoxides. Meepowpan and co-workers have proposed a method for synthesizing soluble liquid $Sn(OR)_2$ using stoichiometric amounts of anhydrous tin(II) chloride $(SnCl_2)$, diethylamine $((C_2H_5)_2NH)$, and an alcohol (ROH).[17] Because the liquid $Sn(OR)_2$ is completely soluble, it leads to more reproducible results which, in turn, leads to a more detailed understanding of the kinetics and mechanism of the ROP reaction. Using the $Sn(OR)_2$ initiator directly instead of generating it *in situ* should give more reproducible and predictable results in terms of both kinetic and molecular weight control compared with the $Sn(Oct)_2/ROH$ initiating system or $Sn(Oct)_2$ alone.

In order to investigate the efficiency of the liquid tin(II) alkoxide initiators, the kinetics of the ROP of LA were investigated by measuring the decrease in the monomer concentration
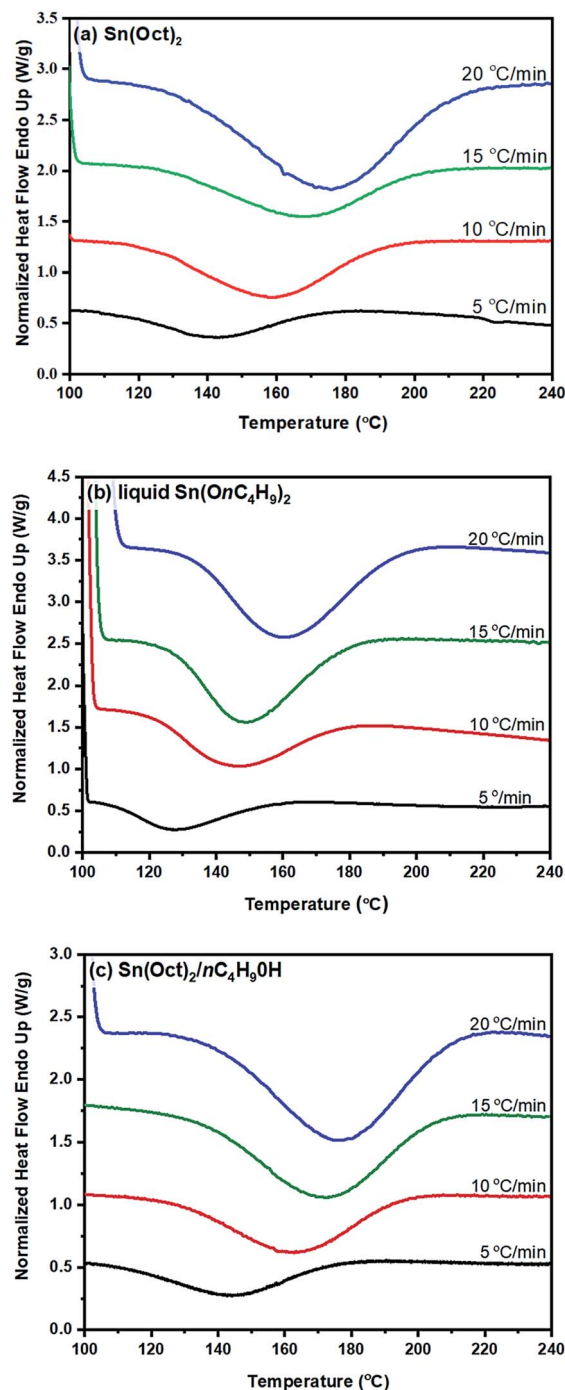
Fig. 5 DSC thermograms of normalized heat flow (W g^{-1}) against temperature (°C) for the ROP of L-lactide using: (a) 1.0 mol% $Sn(Oct)_2$; (b) 1.0 mol% liquid $Sn(OnC_4H_9)_2$; and (c) 1.0/2.0 mol% $Sn(Oct)_2/nC_4H_9OH$ as initiators and initiating system at heating rates of (−) 5, (−) 10, (−) 15, and (−) 20 °C min^{-1}.

as a function of time. This can be done by a variety of methods such as dilatometry, gravimetry, proton-nuclear magnetic resonance (^{1}H-NMR) spectroscopy, infrared (IR) spectroscopy, Raman spectroscopy, and differential scanning calorimetry (DSC).[18–23]

Among those aforementioned methods, DSC has been found to be a fast and convenient method for studying polymerization
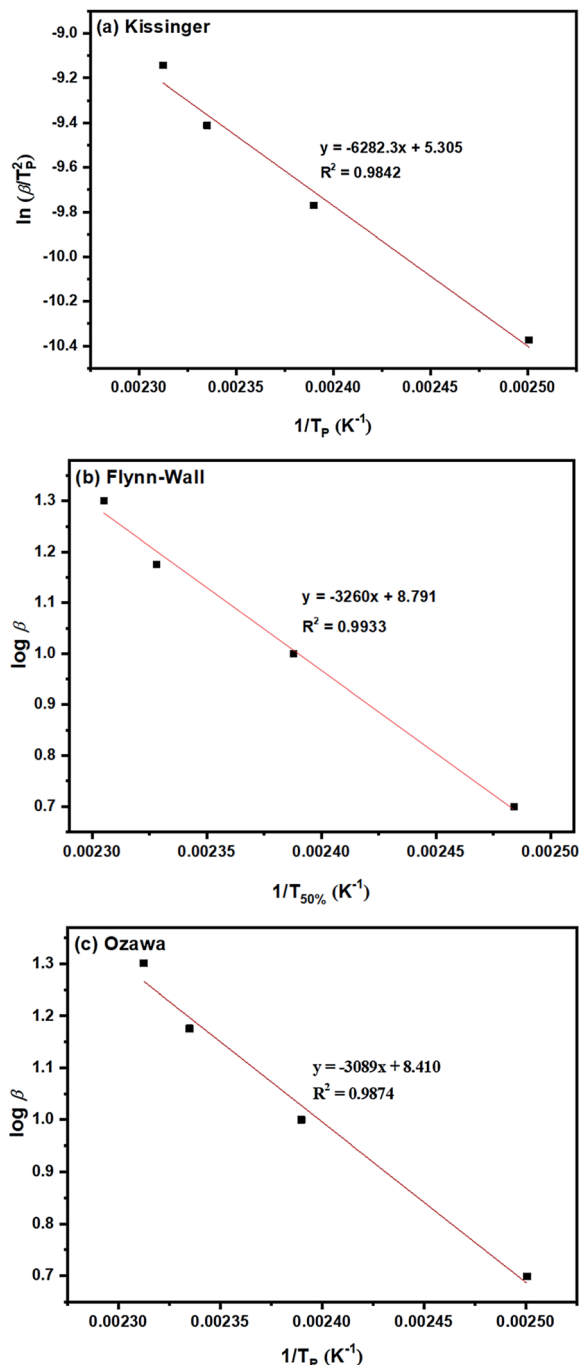
Fig. 6 E_a determinations based on dynamic methods of: (a) Kissinger; (b) Flynn–Wall; and (c) Ozawa for the ROP of L-lactide using 1.0 mol% liquid $Sn(OnC_4H_9)_2$ as an initiator.

kinetics and for determining kinetic parameters such as monomer conversion (α), rate of polymerization ($d\alpha/dt$), order of reaction (n), and activation energy (E_a) of the ROP of both liquid and solid cyclic ester monomers. Furthermore, with the advent of convenient software-based data analysis programs, the ability to obtain such kinetic information has become more practical compared to other techniques.[24–27]

DSC kinetic experiments can be performed under either isothermal or non-isothermal conditions. In isothermal DSC, the polymerization is conducted at a constant temperature while in non-isothermal DSC, polymerization occurs during a temperature scan at a constant heating rate. The conversion of monomer to polymer can be determined from the amount of heat released from the reaction at any time t (ΔH_t) divided by the total heat of reaction (ΔH_m). Then, from the monomer conversion, various kinetic parameters such as rate of polymerization ($d\alpha/dt$), activation energy (E_a), and rate constant (k) can be determined.

However, due to the overlap of the endothermic lactide melting peak and the exothermic peak from its polymerization in isothermal DSC, as reported in previous work,[24] only non-isothermal DSC studies of the ROP of LLA polymerization in bulk were carried out in this work.

2. Experimental

2.1. Purification of L-lactide monomer

Crude L-lactide (Bioplastic Production Laboratory for Medical Applications, ISO 13485:2016 Accredited Laboratory, Chiang Mai University) was purified by repeated (approximately three times) recrystallization from distilled ethyl acetate to yield pure L-lactide as a white, needle-like, crystalline solid. It was then dried to constant weight in a vacuum oven at 55 °C prior to being transferred to a controlled atmosphere glove box (Labconco) for use in synthesis. The final product of >99.9% purity was obtained in a percentage yield of 40–55%.
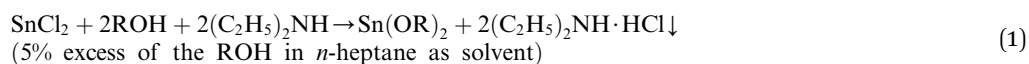
2.2. Purification of $Sn(Oct)_2$ initiator

$Sn(Oct)_2$ (Sigma-Aldrich) was purified by bulb-to-bulb vacuum distillation. Firstly, $Sn(Oct)_2$ was stirred under reduced pressure (high vacuum) at room temperature to remove residual water. Then, the 2-ethylhexanoic acid impurity was removed under vacuum distillation at 120–126 °C/15 Torr (boiling point = 140 °C/23 Torr).[28] The purified $Sn(Oct)_2$ remaining in the heating flask was obtained as a colorless viscous liquid and was stored over molecular sieves type 4 Å.

2.3. Synthesis of liquid tin(II) n-alkoxide initiators

In this work, the synthesis of liquid tin(II) alkoxides for use as initiators in the ROP of L-lactide was as described in the novel modified method by Meepowpan *et al.*[17] and shown in eqn (1):

The synthesis process employed anhydrous tin(II) chloride ($SnCl_2$, Sigma-Aldrich) dissolved in n-heptane (nC_7H_{16}, Sigma-

$$SnCl_2 + 2ROH + 2(C_2H_5)_2NH \rightarrow Sn(OR)_2 + 2(C_2H_5)_2NH \cdot HCl\downarrow$$
$$\text{(5\% excess of the ROH in } n\text{-heptane as solvent)}$$

(1)

Aldrich) mixed with dry diethylamine ($(C_2H_5)_2NH$, Panreac). An alcohol, n-ROH, in which the R group was either $n\text{-}C_4H_9$, $n\text{-}C_6H_{13}$, or $n\text{-}C_8H_{17}$ (Labscan) was added to the reaction mixture and stirred for 12 hours. The reaction mixture of the diethylamine hydrochloride salt, the n-heptane solvent plus any residual alcohol, ROH, and diethylamine was then filtered under a nitrogen atmosphere before being evaporated to dryness. All of the three tin(II) alkoxides, namely: tin(II) n-butoxide ($Sn(OnC_4H_9)_2$), tin(II) n-hexoxide ($Sn(OnC_6H_{13})_2$), and tin(II) n-octoxide ($Sn(OnC_8H_{17})_2$) were obtained as viscous, dark yellow liquids which were readily soluble in most common organic solvents such as chloroform, toluene, and n-heptane. Moreover, they could all be stored under an inert atmosphere for long periods i.e. up to 1 month without any significant change in their reactivity and, therefore, in their efficiency as initiators for the ROP of L-lactide. Fig. 3 shows chemical structures of stannous octoate and the three liquid tin(II) n-alkoxides synthesized in this work.

2.4. Kinetic studies by DSC

Non-isothermal DSC kinetic studies of the ROP of L-LA using the $Sn(Oct)_2$; $Sn(OnR)_2$ initiators and $Sn(Oct)_2/n\text{ROH}$ initiating systems were performed on a PerkinElmer DSC 7 Differential Scanning Calorimeter under a flowing nitrogen (N_2)

atmosphere (20 mL min^{-1}). Prior to measurement, the instrument was calibrated using high purity (>99.999%) indium and tin standards ($T_m = 156.60$ °C, $\Delta H_f = 28.45$ J g^{-1} and $T_m = 231.88$ °C, $\Delta H_f = 60.46$ J g^{-1} respectively).[29,30] The data obtained were analyzed by using Pyris 1 software. For each experiment, 5–10 mg of the well-mixed monomer-initiator sample was weighed into a 50 μL aluminium pan and hermetically sealed. Measurements were performed at heating rates of 5, 10, 15, and 20 °C min^{-1} over the temperature range of 20 to 240 °C. The experimental data were analyzed by the three so-called dynamic; isoconversional; and B/D approaches.

2.4.1. Non-isothermal kinetic analyses of ROP of L-lactide

2.4.1.1. Dynamic methods. In general, the polymerization rate can be described by the following rate eqn (2):

$$\frac{d\alpha}{dt} = kf(\alpha) \tag{2}$$

where $d\alpha/dt$ is the rate of the polymerization reaction; α is the fractional conversion at a specific time t; k is the rate constant; and $f(\alpha)$ is the concentration dependence function of L-lactide or the conversion dependence function.

The dependence of a rate constant (k) on temperature (T) is given by the Arrhenius eqn (3):[31]

Table 2 Summary of T_p, $T_{50\%}$, and E_a values from the DSC dynamic methods of Kissinger; Flynn–Wall; and Ozawa for L-lactide ROP using various initiators/initiating systems at heating rates of: 5, 10, 15, and 20 °C min^{-1}

Initiators/initiating systems	Heating rate, β (°C min^{-1})	T_p (°C)	$T_{50\%}$ (°C)	E_a (kJ mol^{-1}) Kissinger[a]	Flynn–Wall[b]	Ozawa[c]
$Sn(Oct)_2$	5	142.0	141.8	57	65	61
	10	157.8	157.0			
	15	167.3	166.0			
	20	176.0	173.0			
Liquid $Sn(OnC_4H_9)_2$	5	128.9	131.1	52	59	56
	10	145.3	147.2			
	15	150.8	152.5			
	20	160.3	161.7			
$Sn(Oct)_2/nC_4H_9OH$	5	139.2	138.8	60	67	64
	10	152.3	151.7			
	15	161.5	160.3			
	20	170.0	169.0			
Liquid $Sn(OnC_6H_{13})_2$	5	144.8	144.2	57	60	61
	10	157.5	157.1			
	15	170.0	167.3			
	20	177.0	174.3			
$Sn(Oct)_2/nC_6H_{13}OH$	5	148.8	148.5	61	67	66
	10	160.0	159.0			
	15	174.3	173.3			
	20	179.3	178.0			
Liquid $Sn(OnC_8H_{17})_2$	5	152.3	152.8	65	71	69
	10	168.5	167.3			
	15	175.5	175.8			
	20	185.3	184.0			
$Sn(Oct)_2/nC_8H_{17}OH$	5	160.3	158.3	71	74	72
	10	169.3	168.0			
	15	177.5	176.5			
	20	187.0	186.7			

[a] Kissinger: $d[\ln(\beta/T_p^2)]/d(1/T_p) = -E_a/R = $ slope. [b] Flynn–Wall: $\log g(\alpha) = \log(Af(\text{cat})E_a/R) - \log \beta - 2.315 - 0.457(E_a/RT_{50\%})$, slope $= -0.457(E_a/R)$. [c] Ozawa: $\log \beta = $ constant $- 0.4567(E_a/RT_p)$, slope $= -0.4567(E_a/R)$.

$$k = A \exp \left(-\frac{E_a}{RT} \right) \tag{3}$$

where A is a pre-exponential or "frequency" factor (min^{-1}); E_a is the activation energy ($J\ mol^{-1}$); R is the gas constant = 8.314 J $mol^{-1}\ K^{-1}$; and T is the temperature (K).

The activation energy (E_a) of the polymerization reaction can be determined by using peak methods which consider using the peak temperature at maximum rate (T_p) such as the Kissinger and Ozawa methods and using the temperature at 50% conversion ($T_{50\%}$) such as the Flynn–Wall method. The Kissinger, Flynn–Wall, and Ozawa methods are DSC dynamic methods which rely on approximating the so-called temperature integral and require data on temperature only.[32,33]

The Kissinger method uses the temperature at which the rate of polymerization is at the maximum (T_p) and the activation energy, E_a, is obtained from the maximum reaction rate where $d(d\alpha/dt)/dt$ is zero under a constant heating rate condition leading to eqn (4) as follows:[34,35]

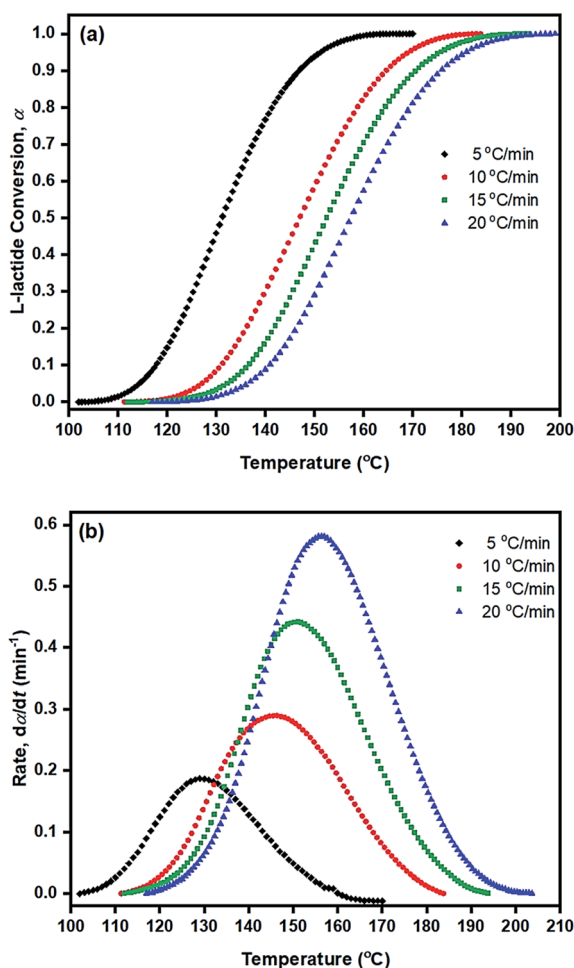$$\ln \left(\frac{\beta}{T_p^2} \right) = \ln \left(\frac{AR}{E_a} \right) - \frac{E_a}{RT_p} \tag{4}$$

where β is the constant heating rate which equals dT/dt (K min^{-1}) and T_p is the peak temperature at which the maximum polymerization rate occurs. Therefore, E_a and A can be obtained from the slope and intercept of the linear fit from a plot of $\ln(\beta/T_p^2)$ against $1/T_p$.

The Flynn–Wall method is an integral method for determining the activation energies without any reaction order.[36] This method combining with Doyle's approximation leads to eqn (5):[37]

Fig. 7 Plots of (a) fraction of conversion (α) and (b) rate of polymerization ($d\alpha/dt$, min^{-1}) against temperature (°C) for the ROP of L-lactide using 1.0 mol% liquid $Sn(OnC_4H_9)_2$ as an initiator at heating rates of: (◆) 5; (●) 10; (■) 15; and (▲) 20 °C min^{-1}.
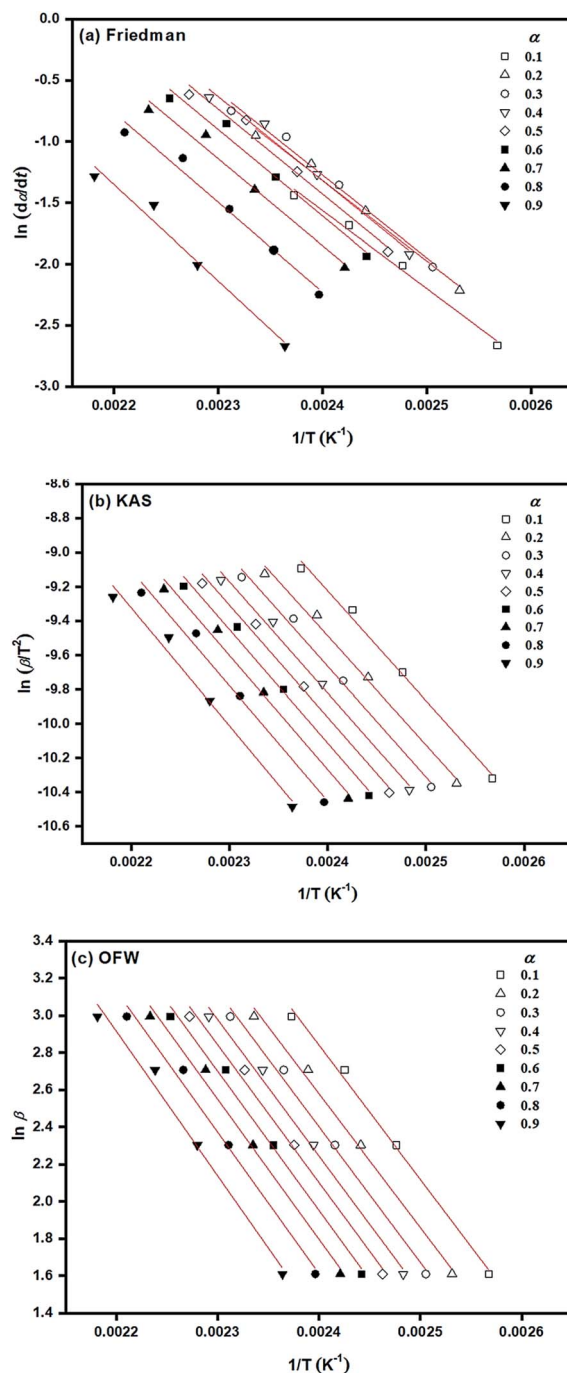

Fig. 8 Determination of E_a based on isoconversional methods of: (a) Friedman; (b) KAS; and (c) OFW for the ROP of L-lactide using 1.0 mol% liquid $Sn(OnC_4H_9)_2$ as an initiator.

Table 3 Summary of E_a ranges from DSC isoconversional methods for ROP of L-lactide using various initiators/initiating systems at heating rates of 5, 10, 15, and 20 °C min^{-1}

Initiator/initiating system	E_a range (kJ mol^{-1})		
	Friedman[a]	KAS[b]	OFW[c]
$Sn(Oct)_2$	58–63	59–74	63–77
$Sn(OnC_4H_9)_2$	53–60	55–58	60–62
$Sn(Oct)_2/nC_4H_9OH$	56–63	56–64	60–67
$Sn(OnC_6H_{13})_2$	56–61	56–60	60–64
$Sn(Oct)_2/nC_6H_{13}OH$	60–63	63–71	67–74
$Sn(OnC_8H_{17})_2$	66–76	66–72	70–76
$Sn(Oct)_2/nC_8H_{17}OH$	68–81	65–74	69–78

[a] Friedman: $\ln (d\alpha/dt) = \ln (Af(\alpha)) - (E_a/RT)$, slope $= -E_a/R$. [b] KAS: $\ln (\beta/T^2) = \ln [(AR)/E_a] - \ln g(\alpha) - E_a/RT$, slope $= -E_a/R$. [c] OFW: $\ln \beta = \ln [(AE)/R] - \ln g(\alpha) - 5.331 - 1.052 (E_a/RT)$, slope $= 1.052 (-E_a/R)$.
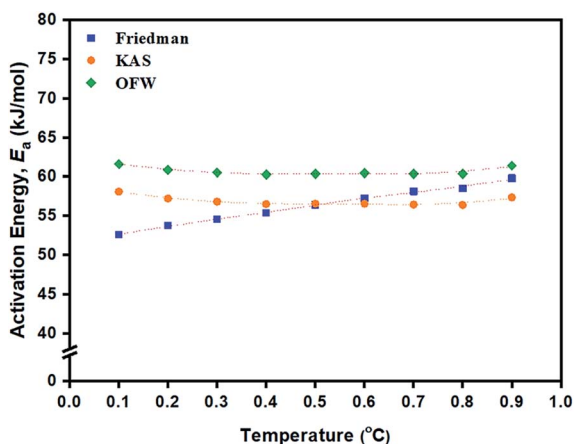
$$\log \, g \, (\alpha) = \log \left[\frac{Af(\text{cat})E_a}{R}\right] - \log \beta - 2.315 - 0.457 \frac{E_a}{RT_{50\%}} \quad (5)$$

where $g(\alpha)$ is an integral conversion dependence function. From eqn (5), E_a can then be obtained from a plot of $\log \beta$ against $1/T_{50\%}$ at a constant $g(\alpha)$. Therefore, activation energy E_a determination from dynamic DSC polymerization only requires determining the temperature at which 50% polymerization is achieved.

Similar to the Flynn–Wall method, the Ozawa method uses the temperature at which the rate of polymerization is at the maximum which, when combined with Doyle's approximation, leads to eqn (6):[38]

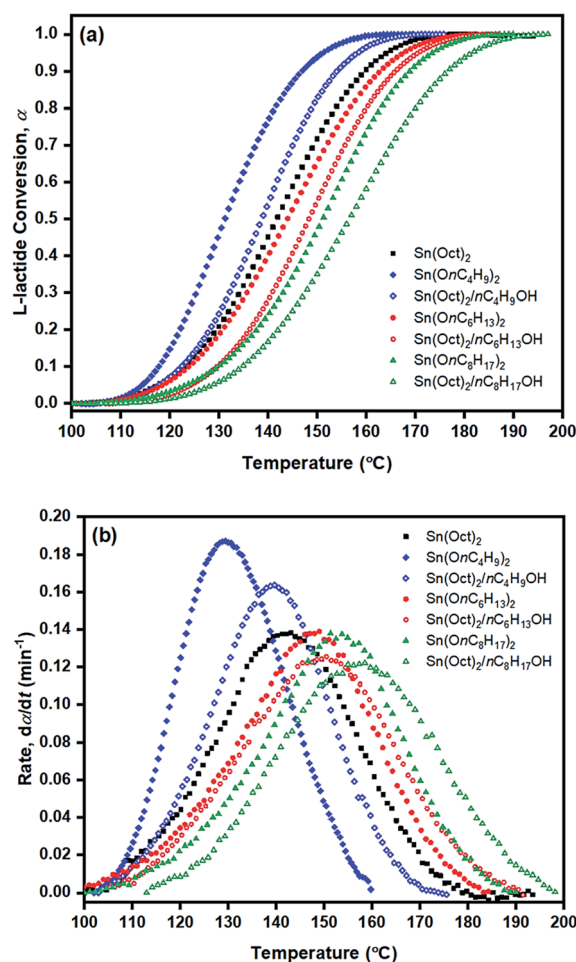$$\log \beta = \text{constant} - 0.4567 \frac{E_a}{RT_p} \quad (6)$$

In this method, plots of $\log \beta$ against $1/T_p$ are used to determine the energy of activation (E_a) from the slopes.

2.4.1.2. Isoconversional methods. Isoconversional methods are amongst the most reliable methods for the calculation of activation energy of thermally activated reactions. Isoconversional methods can be categorized into two main groups of methods.[33] The first group are considered as Type A methods (or rate-isoconversional methods). A well-known method of this type is the Friedman method which makes no mathematical approximations. The second group are considered as Type B methods which apply a range of approximations for the temperature integral $p(x)$ such as the Kissinger–Akahira–Sunose (KAS) method and the Flynn–Wall–Ozawa method.[36,38–40]

These isoconversional methods employ multiple temperature programs (*e.g.*, different heating rates) in order to obtain data from various rates at a constant fraction of conversion (extent of reaction), α. In other words, isoconversional methods allow complex (*i.e.*, multi-step) processes to be determined *via* a variation in activation energy (E_a) with conversion α.[41] This means that, if a significant variation in E_a occurs with conversion α, the process is complex. On the other hand, if E_a is independent of conversion α, then the reaction is a single-step

Fig. 9 Dependence of activation energy (E_a, kJ mol^{-1}) on the fraction of conversion (α) from the data obtained from the: (■) Friedman; (●) KAS; and (◆) OFW isoconversional methods for the ROP of L-lactide using 1.0 mol% liquid $Sn(OnC_4H_9)_2$ as an initiator.

Fig. 10 Plots of (a) monomer conversion (α) and (b) rate (dα/dt) against temperature (°C) for L-lactide ring-opening polymerization using various initiators/initiating systems at a heating rate of 5 °C min^{-1}.

process. Isoconversional methods are based exclusively on dynamic DSC analysis.

Based on eqn (2) and (3), the kinetic approach proposed by Friedman expresses the logarithm of reaction rate, $\ln (d\alpha/dt)$, as a function of the reciprocal temperature, as shown in eqn (7).[42] This enables the activation energy E_a to be determined for each fraction of conversion, α:

$$\ln \left(\frac{d\alpha}{dt}\right) = \ln (Af(\alpha)) - \frac{E_a}{RT} \qquad (7)$$

This equation implies that the reaction rate is only a function of temperature at a constant value of α. It is obvious that if the function $f(\alpha)$ is constant for a particular value of α, then $\ln (Af(\alpha))$ is constant as well. Therefore, by plotting $\ln (d\alpha/dt)$ against $1/T$, a value for $-E_a/R$, and hence E_a, can be obtained.

The Kissinger–Akahira–Sunose (KAS) method is based on eqn (8) as follows:

$$\ln \left(\frac{\beta}{T^2}\right) = \ln \left(\frac{AR}{E_a}\right) - \ln g(\alpha) - \frac{E_a}{RT} \qquad (8)$$

The activation energy E_a can then be obtained from the slope of a semi-log plot of $\ln (\beta/T^2)$ against $1/T$ at constant conversion.

The Ozawa–Flynn–Wall (OFW) isoconversional method uses Doyle's approximation leading to eqn (9):[43,44]

$$\ln \beta = \ln \left(\frac{AE}{R}\right) - \ln g(\alpha) - 5.331 - 1.052 \left(\frac{E_a}{RT}\right) \qquad (9)$$

2.4.1.3. Borchardt and Daniels method.[45–48] The Borchardt and Daniels (B/D) approach gives the calculation of activation energy (E_a), pre-exponential factor (A), heat of reaction (ΔH), reaction order (n), and rate constant (k) from a single DSC scan.[45–48] This approach assumes that the reaction follows n^{th} order kinetics and obeys the general rate eqn (10):

$$\frac{d\alpha}{dt} = k(T)(1 - \alpha)^n \qquad (10)$$

where $d\alpha/dt$ = reaction rate (min^{-1}); α = fractional conversion; $k(T)$ = specific rate constant at temperature T; and n = reaction order. The B/D approach also assumes Arrhenius behavior as mentioned previously in eqn (3). Substituting eqn (3) into eqn (10), rearranging, and taking logarithms yields:

$$\frac{d\alpha}{dt} = A \exp \left(\frac{E_a}{RT}\right)(1 - \alpha)^n \qquad (11)$$

Table 4 Summary of activation energy (E_a), Arrhenius pre-exponential factor (A), and apparent polymerization rate constant at 150 °C ($k_{app, 150 °C}$) estimated from Borchardt and Daniels (B/D) approach using various initiators/initiating systems at heating rates of 5, 10, 15, and 20 °C min^{-1}

Initiators/initiating systems	Heating rate, β (°C min^{-1})	Kinetic parameters		
		$E_a{}^a$ (kJ mol^{-1})	A^b (min^{-1})	$k_{app, 150 °C}{}^c$ (min^{-1})
Sn(Oct)$_2$	5	79	5.42×10^{10}	0.3150
	10	89	2.35×10^9	0.3162
	15	89	1.49×10^9	0.3747
	20	91	6.32×10^8	0.4163
Liquid Sn(OnC$_4$H$_9$)$_2$	5	76	3.40×10^{10}	0.5057
	10	78	2.65×10^{10}	0.5742
	15	80	2.19×10^{10}	0.6729
	20	84	2.87×10^{10}	0.7696
Sn(Oct)$_2$/nC$_4$H$_9$OH	5	78	7.82×10^9	0.4230
	10	84	2.59×10^{10}	0.4322
	15	87	3.05×10^{10}	0.4346
	20	88	2.57×10^{10}	0.4936
Liquid Sn(OnC$_6$H$_{13}$)$_2$	5	80	2.63×10^{11}	0.2323
	10	87	3.40×10^{11}	0.2352
	15	87	2.19×10^{11}	0.2458
	20	87	2.07×10^{11}	0.2773
Sn(Oct)$_2$/nC$_6$H$_{13}$OH	5	89	3.64×10^{11}	0.1710
	10	90	3.79×10^{11}	0.1722
	15	92	4.63×10^{11}	0.1975
	20	94	1.13×10^9	0.2172
Liquid Sn(OnC$_8$H$_{17}$)$_2$	5	90	3.52×10^{11}	0.1446
	10	91	4.36×10^9	0.1475
	15	96	9.56×10^9	0.1617
	20	97	9.48×10^9	0.1639
Sn(Oct)$_2$/nC$_8$H$_{17}$OH	5	97	7.66×10^8	0.0372
	10	98	3.44×10^9	0.0943
	15	98	7.84×10^{10}	0.1077
	20	100	1.27×10^{10}	0.1082

^{a} B/D: multiple linear regression of eqn (12), $-E_a/R$ = slope. ^{b} $\ln (A)$ = intercept. ^{c} k_{app} = apparent rate constant at 150 °C = $d\alpha/dt/(1 - \alpha)^n$.

$$\ln\left[\frac{d\alpha}{dt}\right] = \ln(A) + n\ln(1-\alpha) - \frac{E_a}{RT} \qquad (12)$$

Eqn (12) can be solved with a multiple linear regression of the general form: $z = a + bx + cy$ (where $z \cong \ln[d\alpha/dt]$; $\ln(A) \cong a$; $b \cong n$; $x \cong \ln[1-\alpha]$; $c \cong -E_a/R$; and $y \cong 1/T$). The values for $d\alpha/dt$; α; and T are experimental parameters obtained from a single linear heating rate DSC experiment scanning through the temperature region of the reaction exotherm as shown in Fig. 4.

In this B/D method, assume a value for $n = 1$, then the value for $\ln[k(T)]$ can be calculated using eqn (13):

$$\ln[k(T)] = \ln[d\alpha/dt] - n\ln[1-\alpha] \qquad (13)$$

Then E_a can be obtained from the slope of a plot of $\ln[k(T)]$ against $1/T$ at constant conversion ($\alpha = 0.1$–0.9).

2.5. Synthesis and characterization of poly(L-lactide) using liquid tin(II) *n*-butoxide as an initiator

In this work, ring-opening polymerization of L-lactide using liquid $Sn(OnC_4H_9)_2$ initiator was conducted in the bulk phase. Prior to polymerization, L-lactide monomer of a purity of >99.5% was dried under vacuum at 55 °C for at least 8 h. All glasswares and apparatus used were dried at 120 °C overnight and cooled in a controlled atmosphere glove box prior to use. For each polymerization, approximately 3 g of purified and dried L-lactide monomer were accurately weighed into a 10 mL round bottom flask with a magnetic stirring bar. Then required concentration of tin(II) *n*-butoxide, $Sn(OnC_4H_9)_2$, initiator in toluene was added. The reaction flask was then sealed and immersed in a silicone oil-bath for 24 h. At the end of the polymerization period, the reaction flask was removed from the oil-bath and allowed to cool to room temperature. After that, the polymerisate was dissolved in chloroform as solvent and the polymer precipitated from solution by dropwise addition with efficient stirring into ice-cooled absolute methanol. The

polymer products obtained were white tough solid and were characterized by the combination of instrumental methods of: FTIR (Bruker Tensor 27 FTIR spectrometer), ^{1}H-NMR (400 MHz Bruker Avance II NMR spectrometer), DSC (PerkinElmer DSC 7 Differential Scanning Calorimeter) and dilute-solution viscometry (Schott-Geräte AVS 300, Ubbelohde viscometer no. 532 00 0c) respectively. Table 1 shows the synthesized polymer codes and conditions used in this work.

3. Results and discussion

3.1. Synthesis of liquid tin(II) *n*-alkoxides

All three synthesized liquid tin(II) *n*-alkoxides products namely: tin(II) *n*-butoxide ($Sn(OnC_4H_9)_2$), tin(II) *n*-hexoxide ($Sn(OnC_6H_{13})_2$), and tin(II) *n*-octoxide ($Sn(OnC_8H_{17})_2$) were obtained as viscous, dark yellow liquids of approximately 70–85% yield. The physical appearances, solubility test results, and structural confirmations by various techniques of these three liquid initiator products were stated elsewhere.[17]

3.2. Kinetic analyses

3.2.1. Dynamic methods. In dynamic methods, DSC thermograms of normalized heat flow (W g^{-1}) against temperature (°C) for L-lactide polymerization using $Sn(Oct)_2$; liquid $Sn(OnC_4H_9)_2$; and $Sn(Oct)_2/nC_4H_9OH$ are compared in Fig. 5(a)–(c). Fig. 6
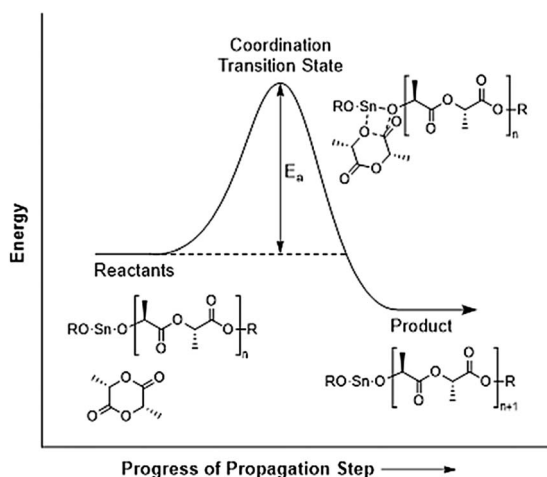

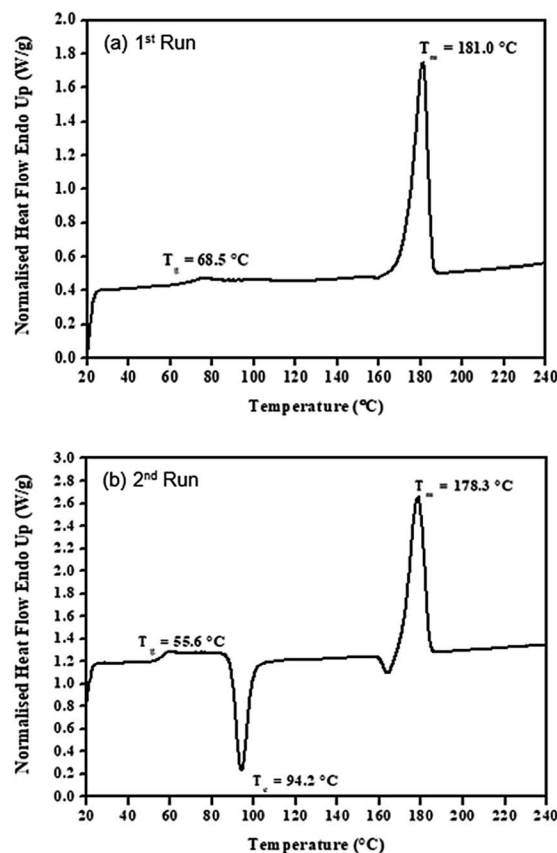Fig. 11 Visualization of the meaning of the value of activation energy, E_a.

Fig. 12 DSC thermograms for (a) 1st run and (b) 2nd run of the purified poly(L-lactide) (PLLA 1) using 0.01 mol% liquid $Sn(OnC_4H_9)_2$ as an initiator at 100 °C for 24 h.

shows activation energy (E_a) determinations based on dynamic methods of: (a) Kissinger; (b) Flynn–Wall; and (c) Ozawa for L-lactide polymerization using liquid tin(II) n-butoxide ($Sn(OnC_4H_9)_2$) as an initiator. Additionally, the peak temperature at the maximum polymerization rate (T_p), the temperature at 50% conversion ($T_{50\%}$), as well as the E_a values from these three dynamic approaches of L-lactide ring-opening polymerization using all the seven initiators/initiating systems are summarized in Table 2.

From the original DSC thermograms of heat flow (normalized, W g^{-1}) against temperature (°C) at the four different heating rates of 5, 10, 15, and 20 °C min^{-1}, it was found that the temperature at the maximum peak (T_p) and the temperature of 50% L-lactide monomer conversion ($T_{50\%}$) were found to increase with increasing heating rate.

However, when considering the initial temperatures (*i.e.* onset temperatures, T_{onset}), it was found that T_{onset} only slightly increased when increasing the heating rate. This observation was seen for almost every initiator/initiating system. Interestingly, the lowest T_{onset} polymerization temperature of ~108 °C was found using the liquid $Sn(OnC_4H_9)_2$ initiator (Fig. 5(b)) indicating its potential as an initiator to synthesize the PLA at low temperature and yielding the polymer with controlled molecular weight and narrow molecular weight distribution in a short period of time.

Furthermore, the E_a values for the L-lactide polymerizations using the seven initiators/initiating systems can be obtained from the slopes of the plots of (a) ln (β/T_p^2) as a function of $1/T_p$, (b) log β as a function of $1/T_{50\%}$ and (c) log β as a function of $1/T_p$ based on the Kissinger, Flynn–Wall and Ozawa methods respectively. The E_a (kJ mol^{-1}) values obtained from linear equation fitting for these three dynamic methods are compared in Table 2 as previously mentioned.

From the results obtained, the E_a values are seen to be in the order of liquid $Sn(OnC_4H_9)_2$ < $Sn(Oct)_2/nC_4H_9OH$ < $Sn(Oct)_2$ ≅ liquid $Sn(OnC_6H_{13})_2$ < $Sn(Oct)_2/nC_6H_{13}OH$ ≅ liquid $Sn(OnC_8H_{17})_2$ < $Sn(Oct)_2/nC_8H_{17}OH$.

3.2.2. Isoconversional methods. For the isoconversion methods, selected plots of the fraction of conversion (α) and rate of polymerization (dα/dt, min^{-1}) against temperature (°C) for the ROP of L-lactide using liquid $Sn(OnC_4H_9)_2$ as an initiator at heating rates of 5, 10, 15, and 20 °C min^{-1} are shown in Fig. 7(a) and (b). It can be seen from Fig. 7 that both the conversion and the rate of polymerization plots against temperature are shifted to higher temperature with increasing heating rate.

According to isoconversional methods, values of E_a of the ROP of L-lactide were determined from the non-isothermal DSC data by the three methods of Friedman, KAS, and OFW. The plots of

Table 5 Summary of values on DSC thermal transition temperatures (T_g, T_c, and T_m), heats of crystallisation (ΔH_c), and heats of melting (ΔH_m) of all synthesized PLLAs using liquid $Sn(OnC_4H_9)_2$ as an initiator for 24 h

Polymer code	T_g (°C)		T_c (°C)		T_m (°C)		ΔH_c (J g^{-1})		ΔH_m (J g^{-1})	
	1st	2nd	1st	2nd	1st	2nd	1st	2nd	1st	2nd
PLLA 1	68.5	56.6	—	94.2	181.0	178.3	—	41.0	64.1	76.0
PLLA 2	67.0	54.3	—	98.8	178.0	175.5	—	40.4	64.5	70.5
PLLA 3	69.9	55.6	—	103.0	179.8	179.5	—	38.6	46.4	56.1
PLLA 4	68.6	59.8	—	106.8	177.8	177.7	—	34.2	38.0	45.9
PLLA 5	63.7	58.7	—	108.8	176.0	175.7	—	40.5	43.3	47.1
PLLA 6	—	59.1	—	105.3	176.5	176.8	—	36.2	42.2	50.9
PLLA 7	54.2	51.6	—	95.2	178.5	174.8	—	38.6	72.1	68.1
PLLA 8	69.9	55.2	—	118.0	178.7	177.0	—	53.6	52.5	47.5
PLLA 9	68.6	55.8	—	106.7	178.2	178.7	—	39.3	52.3	46.4
PLLA 10	72.3	60.1	—	108.7	178.8	178.8	—	32.1	34.1	36.9
PLLA 11	—	57.6	—	106.7	174.3	174.5	—	35.9	41.2	43.2
PLLA 12	71.0	59.1	—	107.5	176.0	176.5	—	36.6	43.2	41.5
PLLA 13	68.3	43.4	—	90.2	176.2	168.2	—	40.0	60.5	55.7
PLLA 14	67.0	51.7	—	99.3	177.2	173.9	—	37.8	64.0	56.1
PLLA 15	69.4	54.8	—	106.2	176.0	176.5	—	43.2	44.8	46.6
PLLA 16	71.7	60.2	—	109.3	179.5	180.2	—	35.1	39.0	45.6
PLLA 17	70.3	57.1	—	112.2	171.7	171.0	—	42.4	43.5	38.5
PLLA 18	69.0	58.2	—	108.2	174.2	176.2	—	37.0	51.6	40.2
PLLA 19	62.6	42.1	—	80.2	166.5	160.8	—	37.6	67.7	56.8
PLLA 20	60.4	39.6	—	86.3	169.3	163.7	—	40.4	63.4	47.5
PLLA 21	68.1	40.2	—	85.2	175.0	167.3	—	37.2	56.0	53.8
PLLA 22	74.7	48.8	—	95.0	175.5	169.0	—	38.5	50.5	48.1
PLLA 23	70.7	45.4	—	91.7	173.0	166.5	—	34.6	49.8	43.0
PLLA 24	—	43.9	—	87.3	173.3	166.0	—	31.6	49.3	45.2
PLLA 25	—	36.5	—	73.0	164.3	157.7	—	33.7	63.6	47.2
PLLA 26	61.9	37.0	—	77.0	165.0	157.0	—	34.9	67.8	50.3
PLLA 27	—	39.0	—	78.8	171.5	164.2	—	33.6	60.1	53.9
PLLA 28	75.6	38.8	—	78.8	172.3	162.3	—	27.3	49.3	45.3
PLLA 29	—	43.6	—	83.5	171.8	163.0	—	31.0	51.0	45.2
PLLA 30	69.4	41.9	—	80.8	171.2	163.2	—	29.1	50.6	46.8

ln (dα/dt), ln (β/dT^2), and ln β against 1/T (K^{-1}) based on these methods for the ROP of L-lactide using 1.0 mol% liquid Sn(OnC$_4$H$_9$)$_2$ as an initiator are shown in Fig. 8(a)–(c). In general, linear plots were obtained for each of the initiating systems although the Friedman plots showed more scattering of the points than those of the KAS and OFW. The values of E_a at a particular conversion, α, can be obtained from the slopes of these linear plots and the values are summarized in Table 3. Again, the Friedman plots showed more variation in E_a with α than the KAS and OFW plots, indicating that the isoconversional KAS and OFW methods are more suitable for E_a determination in L-lactide polymerization. From Fig. 9, similar smaller E_a variations with α were observed for the KAS and OFW methods with the former being consistently <5 kJ mol^{-1} lower than the latter. The consistency of the E_a values over almost the complete range of conversion is an indication that the coordination–insertion mechanism ring-opening polymerization under the conditions is the sole mechanism which is operational in L-lactide employed in this study.

From Table 3, E_a values were found to be the lowest for the Sn(OnC$_4$H$_9$)$_2$ initiator (E_a = 53–60, 55–58, and 60–62 kJ mol^{-1} for Friedman; KAS; and OFW respectively) and the highest for Sn(Oct)$_2$/nC$_8$H$_{17}$OH (E_a = 68–81, 65–74, and 69–78 kJ mol^{-1} for Friedman, KAS, and OFW respectively). When comparing the results at the same heating rate of 5 °C min^{-1} (see Fig. 10(a) and (b)), the conversion and rate plots showed different values of T_{onset} with different conversions or rates of polymerization in the order of: liquid Sn(OnC$_4$H$_9$)$_2$ > Sn(Oct)$_2$/nC$_4$H$_9$OH > Sn(Oct)$_2$ ≅ liquid Sn(OnC$_6$H$_{13}$)$_2$ > Sn(Oct)$_2$/nC$_6$H$_{13}$OH ≅ liquid Sn(OC$_8$H$_{17}$)$_2$ > Sn(Oct)$_2$/nC$_8$H$_{17}$OH.

3.2.3. Borchardt and Daniels (B/D) method. For B/D method, kinetic parameters E_a and frequency factor A can be obtained from multiple linear regression from the plot of ln [$k(T)$] versus 1/T. Table 4 shows values obtained from ROP of L-lactide using all seven initiators/initiating systems at heating rates of 5, 10, 15, and 20 °C min^{-1} respectively.

Similar to previous dynamic and isoconversional approaches, liquid tin(II) n-butoxide shown to be the most efficient initiator due to its lowest activation energy range (76–84 kJ mol^{-1}) with highest apparent rate constant values.

What the E_a value for L-lactide ring-opening polymerization in bulk means essentially is the E_a value for the propagation step since the number of propagation steps far outnumber the initiation and termination steps. Therefore, the actual meaning of E_a can be visualized as shown in the energy diagram in Fig. 11.

3.3. Synthesis and characterization of poly(L-lactide) using liquid tin(II) n-butoxide as an initiator

From the DSC kinetic studies, liquid tin(II) n-butoxide, Sn(OnC$_4$H$_9$)$_2$, has shown to be the most efficient initiator in terms of rate, therefore, it was chosen for a more detailed study of how it can be used to control molecular weight in the ring-opening polymerizaition in bulk of L-lactide by varying its concentration and also the polymerization temperature (Table 1). From the results obtained, structures of all synthesized poly(L-lactide) products using liquid Sn(OnC$_4$H$_9$)$_2$ as an initiator

Table 6 Dilute-solution viscosity data and calculated viscosity terms in chloroform at 25 ± 0.1 °C for purified poly(L-lactide) (PLLA 9) obtained using 0.05 mol% liquid Sn(OnC$_4$H$_9$)$_2$ as an initiator at 120 °C for 24 h

Concentration (g dL^{-1})	Flow-time (sec)	η_{rel}	η_{sp}	η_{red} (dL g^{-1})
0	132.4	—	—	—
0.2012	207.6	1.567	0.567	2.819
0.4120	301.8	2.278	1.278	3.103
0.6056	423.6	3.198	2.198	3.630
0.8012	562.0	4.243	3.243	4.048

at various conditions were confirmed by FTIR and ^{1}H-NMR respectively.

3.3.1. Temperature transitions and heat of melting by DSC. For the temperature transition determination, all DSC analyses of the poly(L-lactide) were conducted at a heating rate of 10 °C min^{-1} under dry nitrogen (N$_2$) using a Perkin Elmer DSC7 Differential Scanning Calorimeter (Pyris 1 Software). For each measurement, a polymer sample was weighed in the range of 3–5 mg and hermetically sealed in a 50 μL sample pan. Typical DSC thermograms (1st run and 2nd run) for poly(L-lactide) synthesized in this work are illustrated in Fig. 12(a) and (b) respectively showing the polymer's glass transition temperature (T_g), crystallisation temperature (T_c) and melting temperature (T_m). The appearance of the T_c peak in the 2nd run is a result of the slow crystallisability of the PLLA during the intermediate fast cooling step. Consequently, whereas the PLLA at the state of the 1st run was semi-crystalline, at the start of the 2nd run it was largely amorphous, hence the appearance of the cold crystallisation T_c peak.

Information on the DSC thermal transition temperatures (i.e. the glass transition temperature (T_g), the crystallisation temperature (T_c), and the melting temperature (T_m)) as well as the heat of crystallization (ΔH_c) and the heat of melting (ΔH_m) from all synthesized PLLA polymer products were summarized in Table 5.
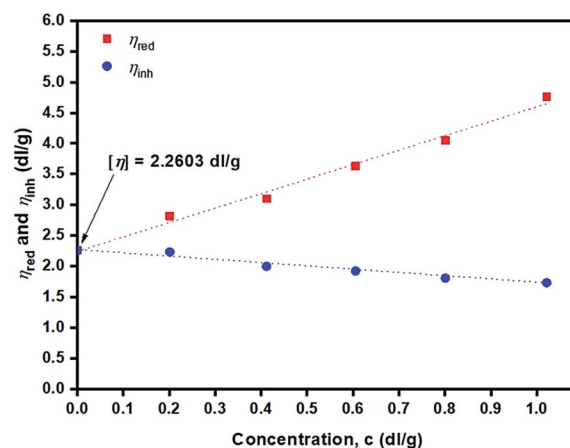
Fig. 13 Plots of reduced viscosity, η_{red} (■) and inherent viscosity, η_{inh} (●) in CHCl$_3$ at 25 ± 0.1 °C against concentration (g dL^{-1}) for purified poly(L-lactide) (PLLA 9) obtained from using 0.05 mol% liquid Sn(OnC$_4$H$_9$)$_2$ as an initiator at 120 °C for 24 h.

3.3.2. Molecular weight determination by dilute-solution viscometry. The viscometric flow-time data and derived viscosity parameters relating to poly(L-lactide) sample synthesised using 0.05 mol% $Sn(OnBu)_2$ at 120 °C for 24 h (PLLA 9) are given in Table 6. The measurement was performed using a Schott-Geräte Ubbelohde viscometer (type no. 532 00 0c) in conjunction with the Schott-Geräte AVS 300 Automatic Viscosity Measuring System. A polymer sample was dissolved in $CHCl_3$ solution at 25 ± 0.1 °C.

Fig. 13 depicts plots of reduced viscosity (η_{red}) and inherent viscosity (η_{inh}) against concentration (g dL^{-1}). Double extrapolating to zero concentration giving a value of intrinsic viscosity [η] of the PLLA sample of 2.26 dL g^{-1} was obtained.

From the value of [η] = 2.26 dL g^{-1} (Fig. 13), the polymer's viscosity-average molecular weight, $\bar{M}_v$, can be calculated from the Mark–Houwink–Sakurada[49] eqn (14) for PLLA in chloroform at 25 ± 0.1 °C:

$$[\eta] = 5.45 \times 10^{-4} \, \bar{M}_v^{-0.73} \text{ dL g}^{-1} \tag{14}$$

$$[2.26] = 5.45 \times 10^{-4} \, \bar{M}_v^{-0.73} \text{ dL g}^{-1}$$

Table 7 Summary on the values of: [η], $\bar{M}_v$ and $\bar{M}_n$ obtained from dilute-solution viscometry for all synthesized PLLAs using liquid tin(II) n-butoxide as an initiator

Polymer code	Intrinsic viscosity, [η] (dL g^{-1})	Viscosity-average molecular weight, $\bar{M}_v$ (g mol^{-1})	Number-average molecular weight, $\bar{M}_n$ (g mol^{-1})
PLLA 1	0.66	2.22×10^4	1.18×10^4
PLLA 2	1.05	3.15×10^4	1.68×10^4
PLLA 3	2.15	8.42×10^4	4.48×10^4
PLLA 4	1.69	6.09×10^4	3.24×10^4
PLLA 5	1.92	7.20×10^4	3.83×10^4
PLLA 6	1.90	7.12×10^4	3.79×10^4
PLLA 7	0.98	2.89×10^4	1.54×10^4
PLLA 8	1.67	5.98×10^4	3.18×10^4
PLLA 9	2.26	9.03×10^4	4.80×10^4
PLLA 10	2.35	9.51×10^4	5.05×10^4
PLLA 11	1.84	6.83×10^4	3.63×10^4
PLLA 12	2.17	8.52×10^4	4.53×10^4
PLLA 13	0.85	2.36×10^4	1.25×10^4
PLLA 14	1.01	2.99×10^4	1.59×10^4
PLLA 15	2.38	9.67×10^4	5.14×10^4
PLLA 16	2.02	7.73×10^4	4.11×10^4
PLLA 17	1.58	5.51×10^4	2.93×10^4
PLLA 18	1.65	5.90×10^4	3.14×10^4
PLLA 19	0.31	6.06×10^3	3.22×10^3
PLLA 20	0.48	1.07×10^4	5.71×10^3
PLLA 21	0.84	2.31×10^4	1.23×10^4
PLLA 22	1.05	3.17×10^4	1.68×10^4
PLLA 23	0.89	2.53×10^4	1.35×10^4
PLLA 24	0.85	2.35×10^4	1.25×10^4
PLLA 25	0.23	4.06×10^3	2.16×10^3
PLLA 26	0.29	5.48×10^3	2.91×10^3
PLLA 27	0.63	1.56×10^4	8.32×10^3
PLLA 28	0.73	1.91×10^4	1.02×10^4
PLLA 29	0.64	1.61×10^4	8.55×10^3
PLLA 30	0.52	1.42×10^4	6.86×10^3

$$\bar{M}_v = 9.03 \times 10^4$$

Therefore, the number-average molecular weight ($\bar{M}_n$), can be calculated from the gamma function[50] eqn (15); assuming an approximately "most probable" molecular weight distribution, as:

$$\frac{\bar{M}_n}{\bar{M}_v} = \frac{1}{[(1+a)\Gamma(1+a)]^{1/a}} \tag{15}$$

where $a = 0.73$ (for PLLA in $CHCl_3$ at 25 °C) and Γ = gamma function, from $\bar{M}_v = 9.03 \times 10^4$, therefore giving:

$$\bar{M}_n = 4.80 \times 10^4 \text{ g mol}^{-1}$$

The values of [η], $\bar{M}_v$, and $\bar{M}_n$ obtained from dilute-solution viscometry for PLLA products were provided in Table 7.

4. Conclusions

In conclusion, these kinetic studies of the ring-opening polymerization of L-lactide in bulk by dynamic (Kissinger; Flynn–Wall; Ozawa), isoconversional (Friedman, KAS, and OFW) and Borchardt and Daniels (B/D) methods have indicated that the efficiency of the various initiators/initiating systems used in this work is in the order of liquid tin(II) n-butoxide ($Sn(OnC_4H_9)_2$) > tin(II) octoate/n-butanol ($Sn(Oct)_2/C_4H_9OH$) > tin(II) octoate ($Sn(Oct)_2$) $\cong$ liquid tin(II) n-hexoxide ($Sn(OnC_6H_{13})_2$) > tin(II) octoate/n-hexanol ($Sn(Oct)_2/nC_6H_{13}OH$) $\cong$ liquid tin(II) n-octoxide ($Sn(OnC_8H_{17})_2$) > tin(II) octoate/n-octanol ($Sn(Oct)_2/nC_8H_{17}OH$).

Therefore, liquid tin(II) n-butoxide ($Sn(OnC_4H_9)_2$) is regarded as being the most efficient initiator for ring-opening polymerization of L-lactide *via* coordination–insertion mechanism as confirmed by the non-isothermal DSC kinetic studies which gave the lowest E_a values and the fastest rates of polymerization at the lowest temperature.

The results also confirm that the use of liquid tin(II) n-alkoxide ($Sn(OR)_2$) initiator directly is more efficient than generating it *in situ via* the $Sn(Oct)_2/ROH$ reaction. It also has the important advantages of (a) knowing the [$Sn(OR)_2$] concentration accurately for the purpose of being able to predict polymerization rates and polymer molecular weights and (b) to avoid any unwanted side-reactions due to the use of $Sn(Oct)_2$ alone and/or $Sn(Oct)_2/ROH$ system.

Conflicts of interest

The authors declare no conflict of interest.

Acknowledgements

Department of Chemistry, Faculty of Science, Chiang Mai University for providing the laboratory facilities.

References

1 J. C. Middleton and A. J. Tipton, *Biomaterials*, 2000, **21**(23), 2335–2346.

2 M. Srisa-ard, R. Molloy, N. Molloy, J. Siripitayananon and M. Sriyai, *Polym. Int.*, 2001, **50**(8), 891–896.

3 Y. Baimark, R. Molloy, N. Molloy, J. Siripitayananon, W. Punyodom and M. Sriyai, *J. Mater. Sci.: Mater. Med.*, 2005, **16**(8), 699–707.

4 W. Channuan, J. Siripitayananon, R. Molloy, M. Sriyai, F. J. Davis and G. R. Mitchell, *Polymer*, 2005, **46**(17), 6411–6428.

5 S. Ruengdechawiwat, J. Siripitayananon, R. Molloy, R. Somsunan, P. D. Topham and B. J. Tighe, *Int. J. Polym. Mater.*, 2016, **65**(6), 277–284.

6 W. H. Carothers, G. L. Dorough and F. J. van Natta, *J. Am. Chem. Soc.*, 1932, **54**(2), 761–772.

7 A. P. Gupta and V. Kumar, *Eur. Polym. J.*, 2007, **43**(10), 4053–4074.

8 W. Groot, J. van Krieken, O. Sliekersl and S. de Vos, Production and Purification of Lactic acid and Lactide, in *Poly(lactic acid) Synthesis, Structures, Properties, Processing, and Applications*, ed. R. Auras, L. Loong-Tak, S. E. M. Selke and T. Hideto, John Wiley & Sons, Inc., Hoboken, New Jersey, 2010, pp. 3–16.

9 O. Dechy-Cabaret, B. Martin-Vaca and D. Bourissou, Polyesters from Dilactones, in *Handbook of Ring-Opening Polymerization* ed. P. Dubois, O. Coulembier and J.-M. Raquez, Wiley-VCH Verlag GmbH & Co. KGaA, Weinheim, 2009, pp. 255–280.

10 H. R. Kricheldorf, K. Bornhorst and H. Hachmann-Thiessen, *Macromolecules*, 2005, **38**(12), 5017–5024.

11 S. Kaihara, S. Matsumura, A. G. Mikos and J. P. Fisher, *Nat. Protoc.*, 2007, **2**(11), 2767–2771.

12 J.-P. Puaux, I. Banu, I. Nagy and G. Bozga, *Macromol. Symp.*, 2007, **259**(1), 318–326.

13 H. R. Kricheldorf, I. Kreiser-Suanders and C. Boettcher, *Polymer*, 1995, **36**(6), 1253–1259.

14 A. Kowalski, A. Duda and S. Penczek, *Macromol. Rapid Commun.*, 1998, **19**(11), 567–572.

15 J. S. Morrison and H. M. Haendler, *J. Inorg. Nucl. Chem.*, 1967, **29**(2), 393–400.

16 R. Gsell and M. Zeldin, *J. Inorg. Nucl. Chem.*, 1975, **37**(5), 1133–1137.

17 P. Meepowpan, W. Punyodom and R. Molloy, Process for the preparation of liquid tin(II) alkoxides, *US Pat.*, 9637507B2, USPTO, USA, 2017.

18 A. Kleawkla, R. Molloy, W. Naksata and W. Punyodom, *Adv. Mater. Res.*, 2008, **55–57**, 757–760.

19 C. Yu, L. Zhang, K. Tu and Z. Shen, *Polym. Bull.*, 2004, **52**(5), 329–337.

20 K. Stridsberg, M. Ryner and A.-C. Albertsson, *Macromolecules*, 2000, **33**(8), 2862–2869.

21 B. Braun, J. R. Dorgan and S. F. Dec, *Macromolecules*, 2006, **39**(26), 9302–9310.

22 S. Parnell, K. Min and M. Cakmak, *Polymer*, 2003, **44**(18), 5137–5144.

23 W. Meelua, R. Molloy, P. Meepowpan and W. Punyodom, *J. Polym. Res.*, 2012, **19**, 9799.

24 R. Mazarro, A. de Lucas, I. Gracia and J. F. Rodriguez, *Macromol. Chem. Phys.*, 2008, **209**(8), 818–824.

25 M. Arasa, X. Ramis, J. M. Salla, A. Mantecón and A. Serra, *Thermochim. Acta*, 2008, **479**(1–2), 37–44.

26 S. Y. Reyes-López and A. M. Richa, *Macromol. Symp.*, 2013, **325–326**(1), 21–37.

27 N. G. Sedush and S. N. Chvalun, *Eur. Polym. J.*, 2015, **62**, 198–203.

28 S.-H. Lee, B.-S. Kim, S. H. Kim, S. W. Choi, S. I. Jeong, I. K. Kwon, S. W. Kang, J. Nikolovski, D. J. Mooney, Y.-K. Han and Y. H. Kim, *J. Biomed. Mater. Res., Part A*, 2003, **66A**(1), 29–37.

29 ASTM standard E967, *Standard Test Method for Temperature Calibration of Differential Scanning Calorimeters and Differential Thermal Analyzers*, ASTM International, West Conshohocken, PA, 2018.

30 ASTM standard E968-02, *Standard Practice for Heat Flow Calibration of Differential Scanning Calorimeters*, ASTM International, West Conshohocken, PA, 2014.

31 K. J. Laidler, *J. Chem. Educ.*, 1984, **61**(6), 494–498.

32 J. H. Flynn, *Thermochim. Acta*, 1997, **300**(1–2), 83–92.

33 M. J. Starink, *Thermochim. Acta*, 2003, **404**(1–2), 163–176.

34 H. E. Kissinger, *J. Res. Natl. Bur. Stand.*, 1956, **57**(4), 217–221.

35 H. E. Kissinger, *Anal. Chem.*, 1957, **29**(11), 1702–1706.

36 J. H. Flynn and L. A. Wall, *J. Polym. Sci., Part C: Polym. Lett.*, 1966, **4**(5), 323–328.

37 C. D. Doyle, *J. Appl. Polym. Sci.*, 1962, **6**(24), 639–642.

38 T. Ozawa, *J. Therm. Anal. Calorim.*, 1970, **2**(3), 301–324.

39 S. Vyazovkin, Isoconversional Methodology, in *Isoconversional Kinetics of Thermally Stimulated Processes*, ed. S. Vyazovkin, Springer International Publishing Switzerland, 2015, pp. 27–62.

40 E. J. Mittemeijer, *J. Mater. Sci.*, 1992, **27**(15), 3977–3987.

41 S. Vyazovkin, *J. Therm. Anal.*, 1997, **49**(3), 1493–1499.

42 H. L. Friedman, *J. Polym. Sci., Part C: Polym. Symp.*, 1964, **6**(1), 183–195.

43 T. Ozawa, *Bull. Chem. Soc. Jpn.*, 1965, **38**(11), 1881–1886.

44 J. H. Flynn and L. A. Wall, *J. Polym. Sci., Part B: Polym. Lett.*, 1966, **4**(5), 323–328.

45 H. J. Borchardt and F. Daniels, *J. Am. Chem. Soc.*, 1957, **79**(1), 41–46.

46 S. J. Swarin and A. M. Wims, *Anal. Calorim.*, 1977, **4**(5), 155–171.

47 ASTM standard E2041, *Standard Test Method for Estimating Kinetic Parameters by Differential Scanning Calorimeters Using the Borchardt and Daniels Method*, ASTM International, West Conshohocken, PA, 2013.

48 R. S. F. Paula, I. M. Figueredo, R. S. Vieira, T. L. Nascimento, C. L. Cavalcante Jr, Y. L. Machado and M. A. S. Rios, *SN Appl. Sci.*, 2019, **1**(884), 1–7.

49 D. R. Witzke and R. Narayan, *Macromolecules*, 1997, **30**(23), 7075–7085.

50 P. J. Flory, Determination of Molecular Weights, in *Principles of Polymer Chemistry*, ed. P. J. Flory, Cornell University Press, Ithaca, New York, 1995, p. 313.